

# Particle Tomography of the Inner Magnetosphere

H. Korth, M. F. Thomsen, and W. S. Phillips

Los Alamos National Laboratory  
Los Alamos, New Mexico, USA

K.-H. Glaßmeier

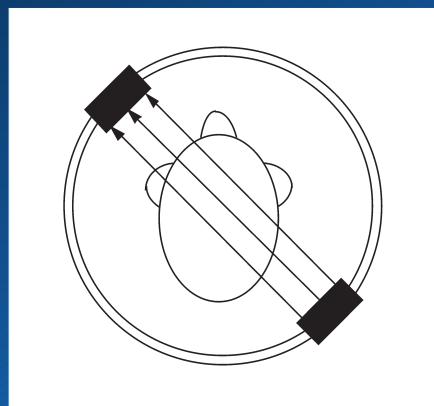
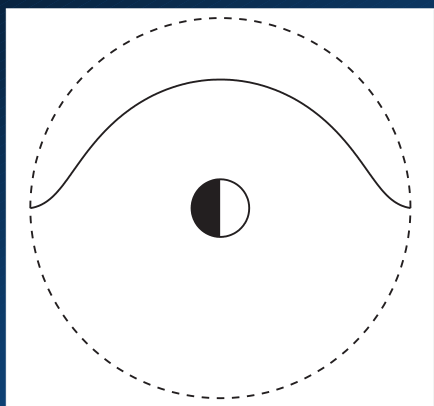
Institut für Geophysik und Meteorologie  
Technische Universität Braunschweig  
Braunschweig, Germany



# Topics

- Particle tomography of the inner magnetosphere.
- Description of parameters.
- Development and test of the inversion algorithm.
- Application to geosynchronous observations.
- Discussion.
- Summary.

# Particle Tomography of the Inner Magnetosphere



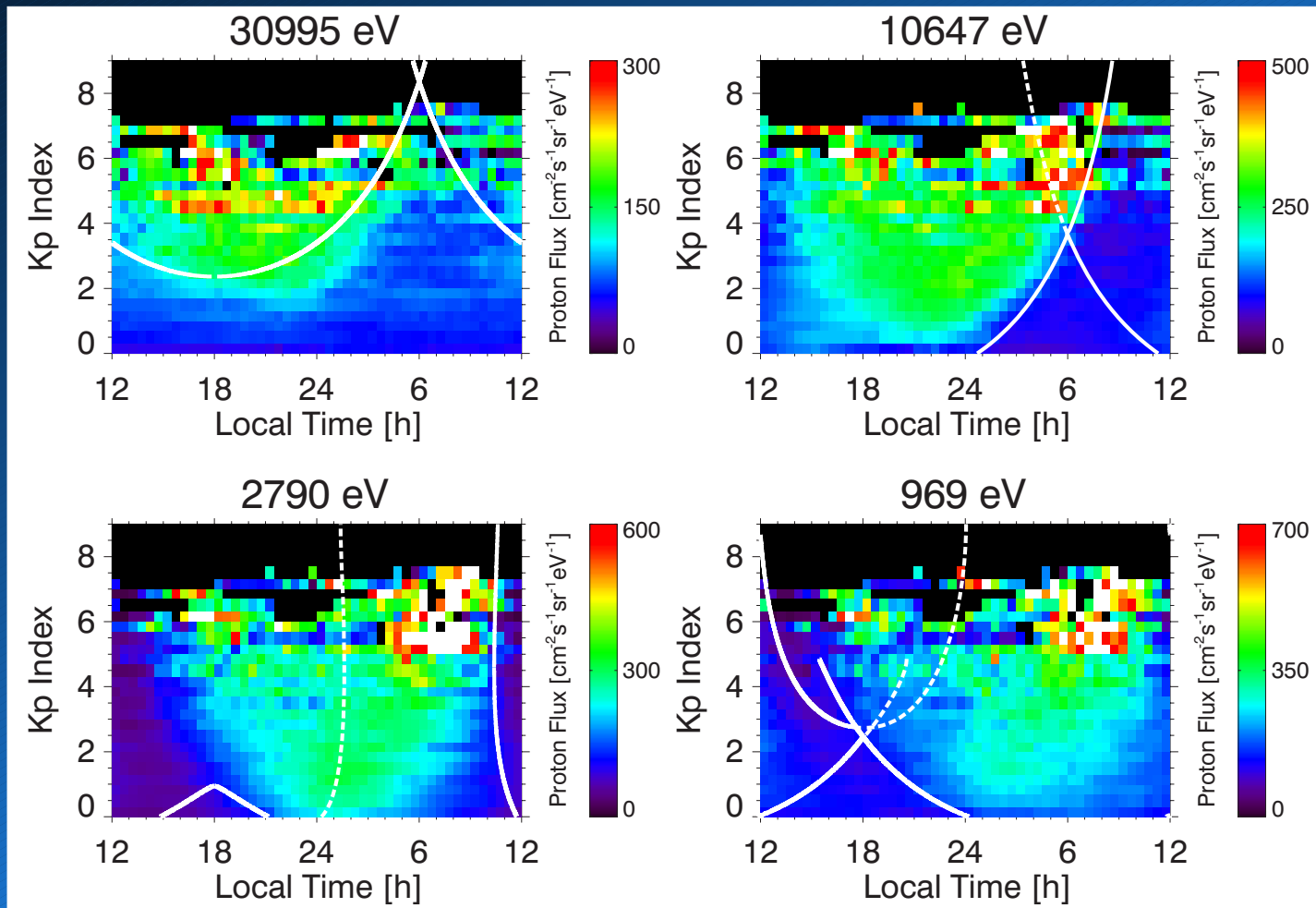
- **Statistics** of the phase space density at geosynchronous orbit.
- The **convection model** provides the trajectories connecting two corresponding data points.
- **Assumption:** Proton losses due to **charge exchange** with exospheric neutral hydrogen.

⇒ Neutral hydrogen distribution by **inversion**.

⇒ Remote-sensing technique known as **tomography**.

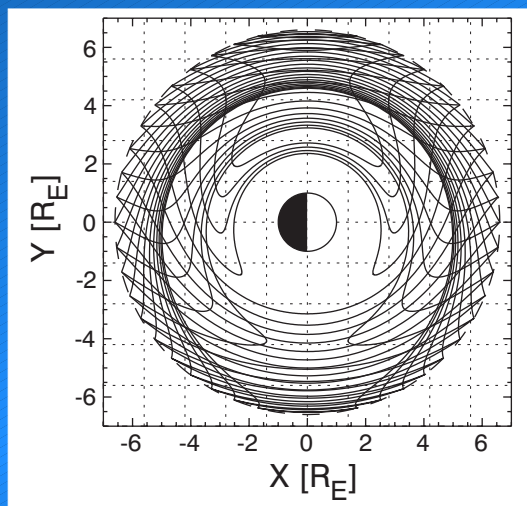


# Geosynchronous Proton Flux Statistics: 1997



# Global Drift Pattern

- A variety of **energies, locations, and Kp levels** lead to a fine mesh of trajectories from the night- to the day-side.
- Dipolar magnetic field.
- Electric potential models:
  - ✓ Volland-Stern (*J. Geophys. Res.*, 595, 1975),
  - ✓ McIlwain E5D (*Adv. Space Res.*, 187, 1986),
  - ✓ Weimer 96 (*Geophys. Res. Lett.*, 2549, 1996).
- Example: Volland-Stern / Dipole drift paths.



# Charge Exchange

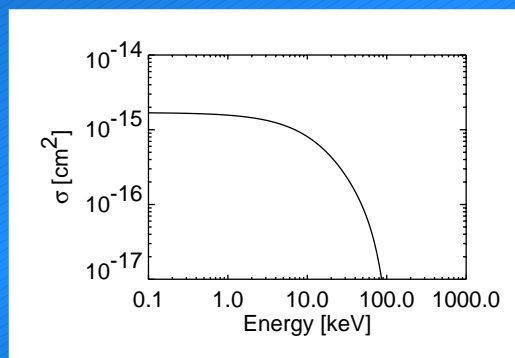
- Liouville's theorem: The phase space density remains constant along the particle trajectory.
- Process:  $H_E^+ + H \rightarrow H_E + H^+$ .
- Decrease of the phase space density  $f$ :

$$v_D \frac{\partial f}{\partial s} = -\sigma v_{th} n_H f$$

$$\Rightarrow f_{out} = f_{in} \exp \left( - \int \sigma v_{th} n_H \frac{ds}{v_D} \right),$$

where  $\sigma$  charge-exchange cross-section,  
 $v_{th}$  thermal speed,  $v_D$  drift speed,  
 $n_H$  neutral hydrogen density.

- The charge-exchange cross-section is energy-dependent:



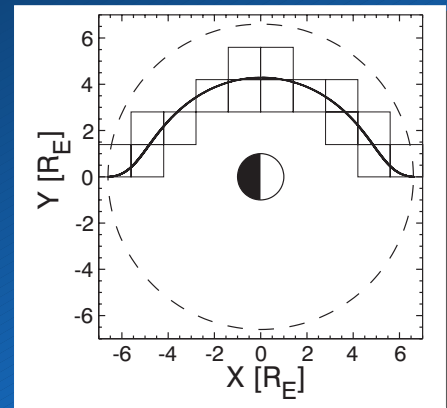


# Tomographic Inversion

- **Discretization** of phase space density decrease:

$$\underbrace{\sum_i \sigma_i v_{th,i} \Delta t_i}_{\mathbf{A}} \underbrace{n_{H,i}}_{\vec{m}} = \underbrace{\ln \left( \frac{f_{in}}{f_{out}} \right)}_{\vec{d}},$$

where  $\mathbf{A}$  contains the drift paths,  
 $\vec{d}$  the PSD ratios, and  
 $\vec{m}$  the neutral densities.



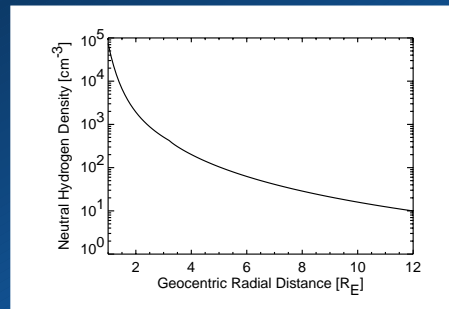
- The matrix  $\mathbf{A}$  is invertible if it is **square** and **regular**.
- Square:  $(\mathbf{A}^T \mathbf{A}) \vec{m} = \mathbf{A}^T \vec{d}$ .
- Regular:  $(\mathbf{A}^T \mathbf{A} + \lambda \mathbf{D}^T \mathbf{D}) \vec{m} = \mathbf{A}^T \vec{d}$ .

⇒ The **neutral density distribution** is given by:

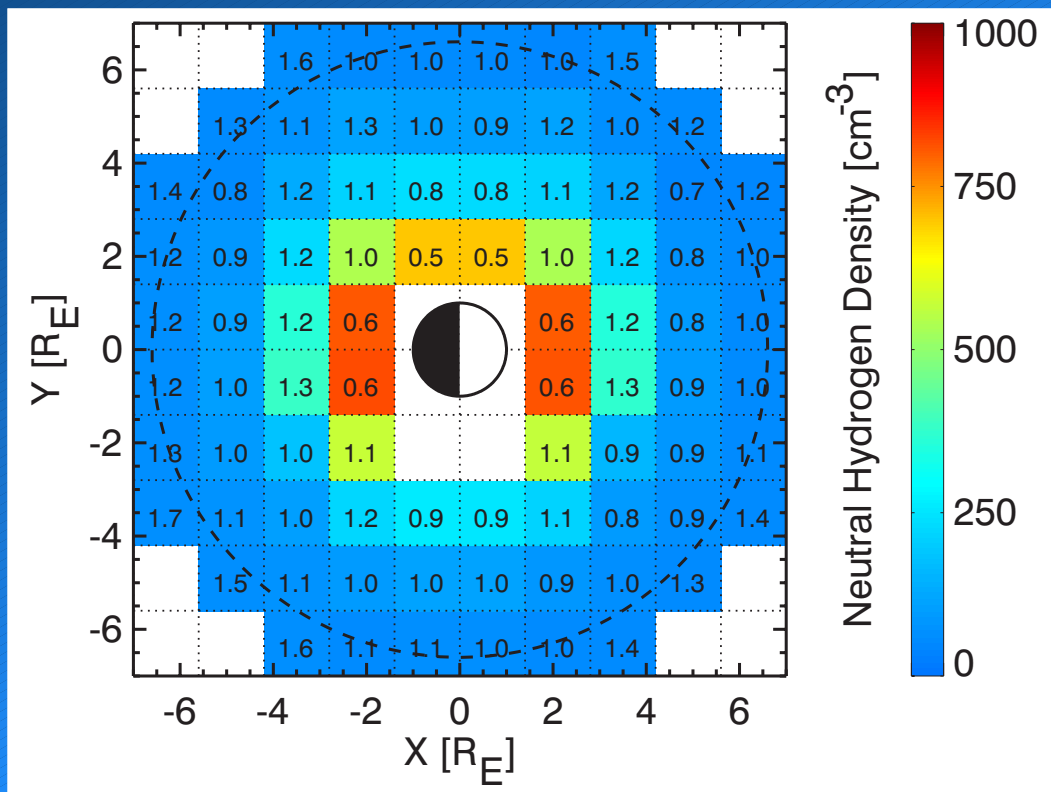
$$\vec{m} = (\mathbf{A}^T \mathbf{A} + \lambda \mathbf{D}^T \mathbf{D})^{-1} \mathbf{A}^T \vec{d}.$$

# Inversion of the Forward Simulation

- Distribution of exospheric neutral hydrogen:  
Chamberlain model with Rairden 86 parameterization.



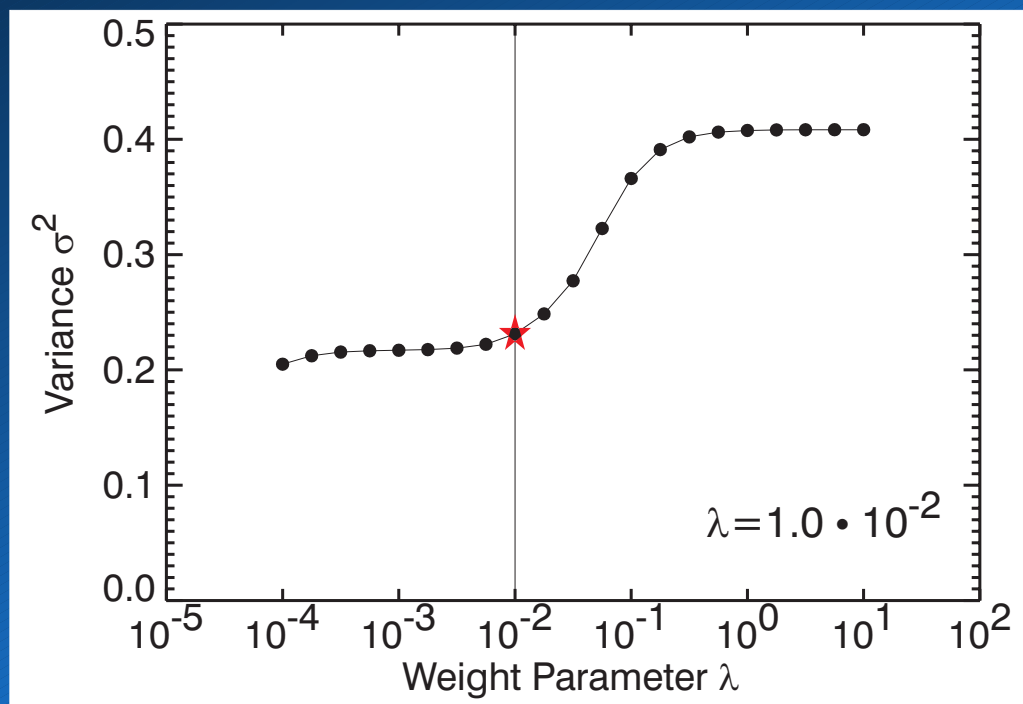
- Inversion of the Forward Simulation:





# The Weight Factor

- Model solution:  $\vec{m} = (\mathbf{A}^T \mathbf{A} + \lambda \mathbf{D}^T \mathbf{D})^{-1} \mathbf{A}^T \vec{d}$ .
- Choice of the weight factor  $\lambda$ :

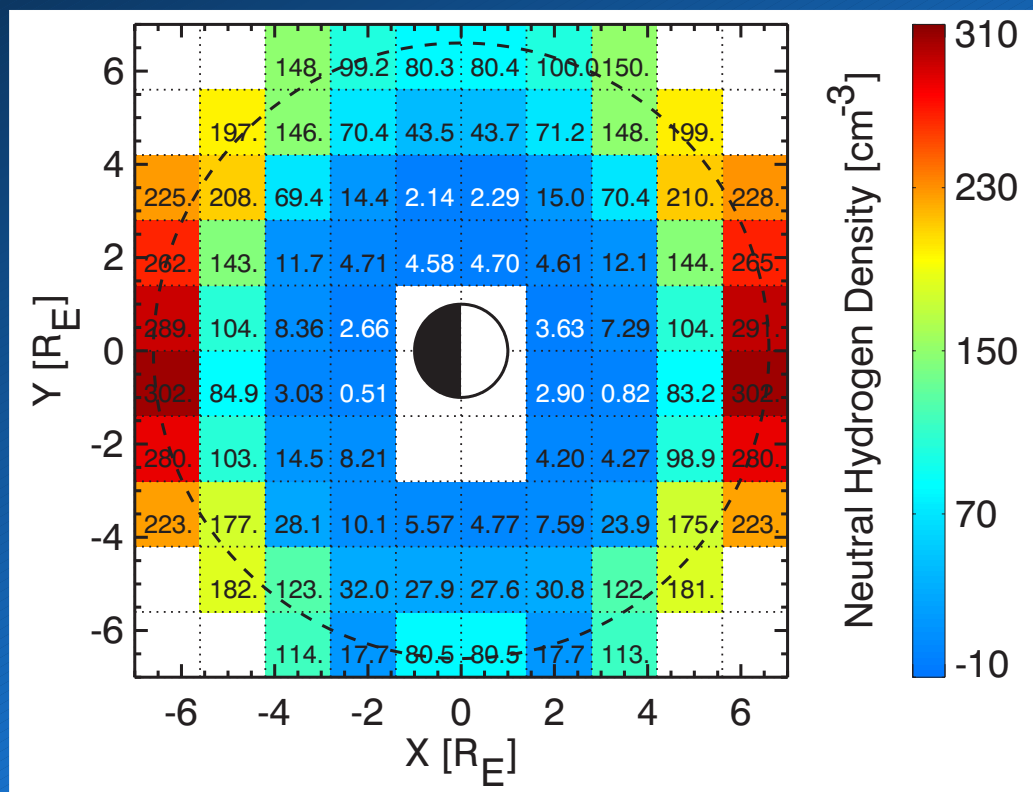


- $\lambda$  too small  $\Rightarrow$  Data noise prevails.
- $\lambda$  too large  $\Rightarrow$  Average density.

# Inversion of the MPA Statistics

(Year: 1997)

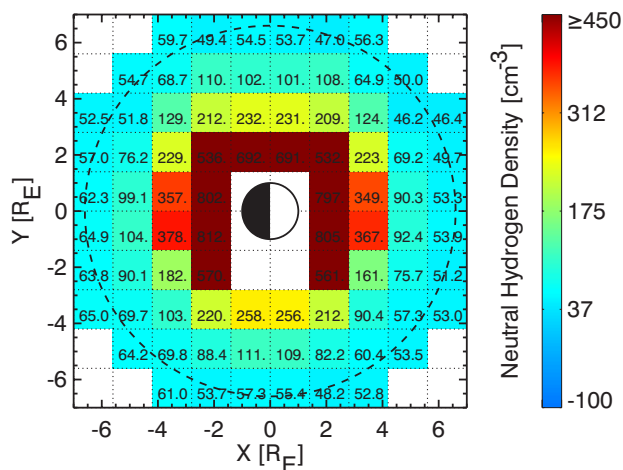
- Volland-Stern electric potential, dipole magnetic field.
- Inverted neutral hydrogen distribution:



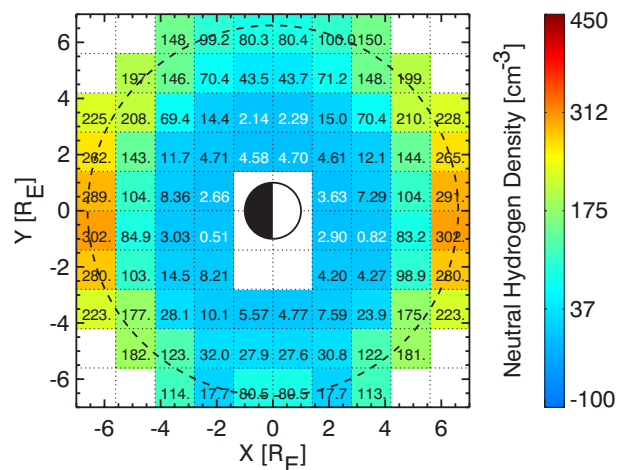
- The inversion shows **near-Earth densities** that are **significantly lower** than predicted by the Chamberlain model.

# Inverted Hydrogen Densities

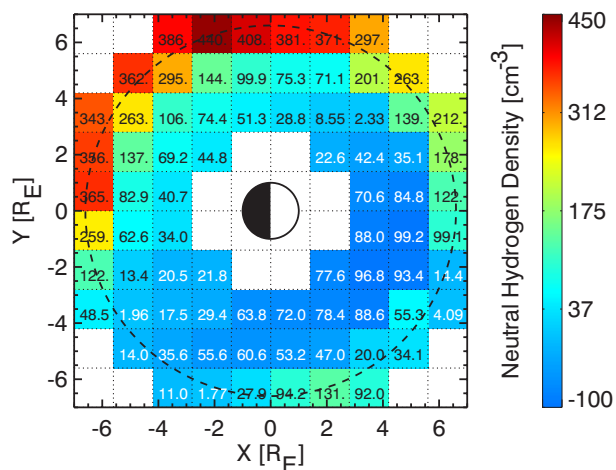
## Volland-Stern



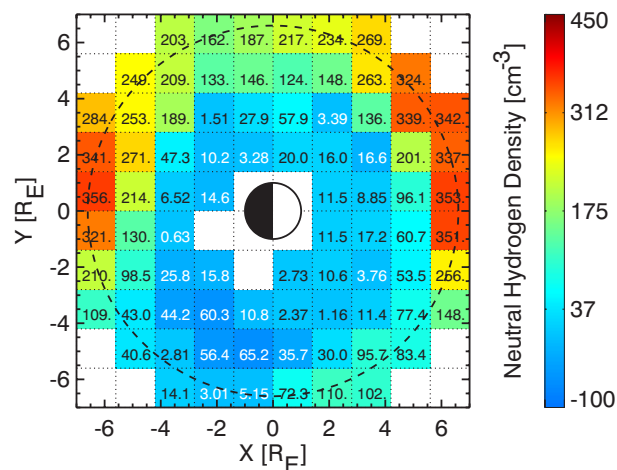
## Volland-Stern



## McIlwain E5D



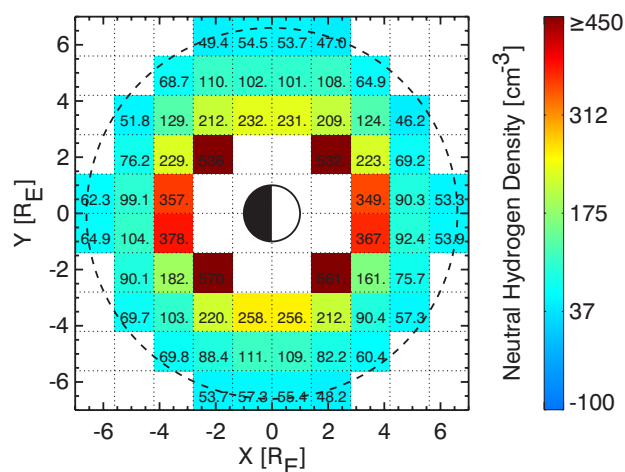
## Weimer 96



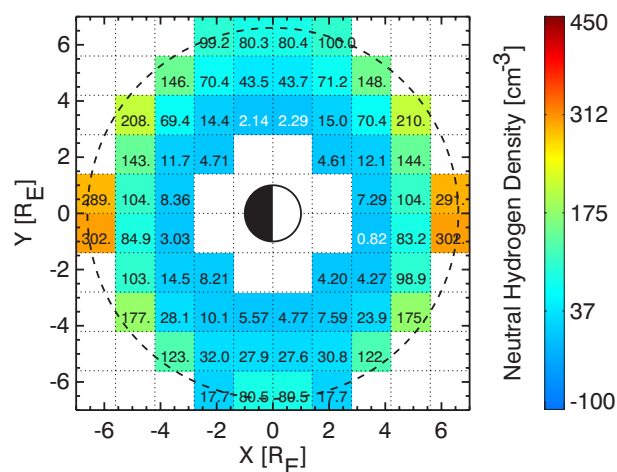


# Inverted Hydrogen Densities (Resolution $\geq 0.2$ )

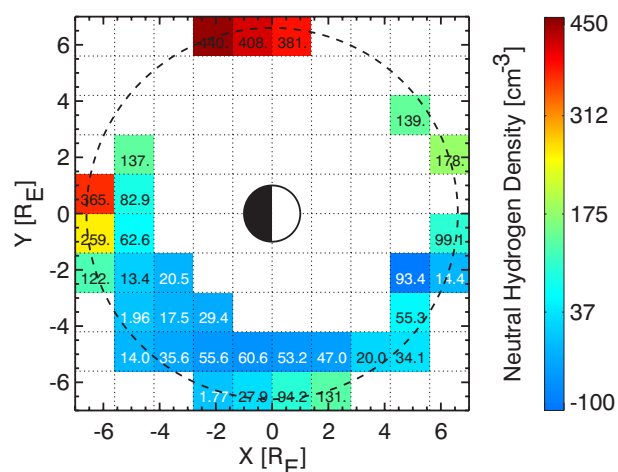
Volland-Stern



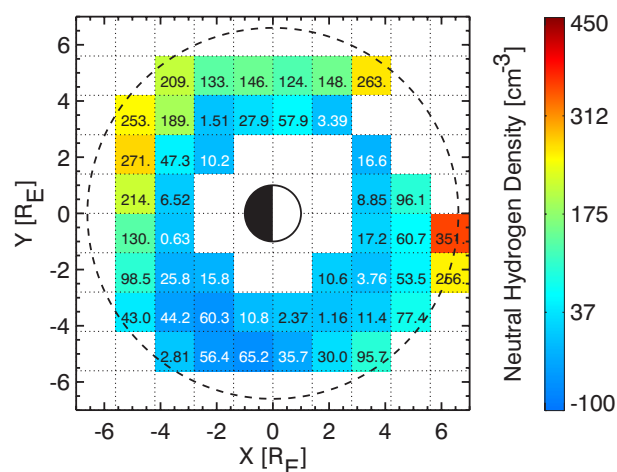
Volland-Stern



McIlwain E5D

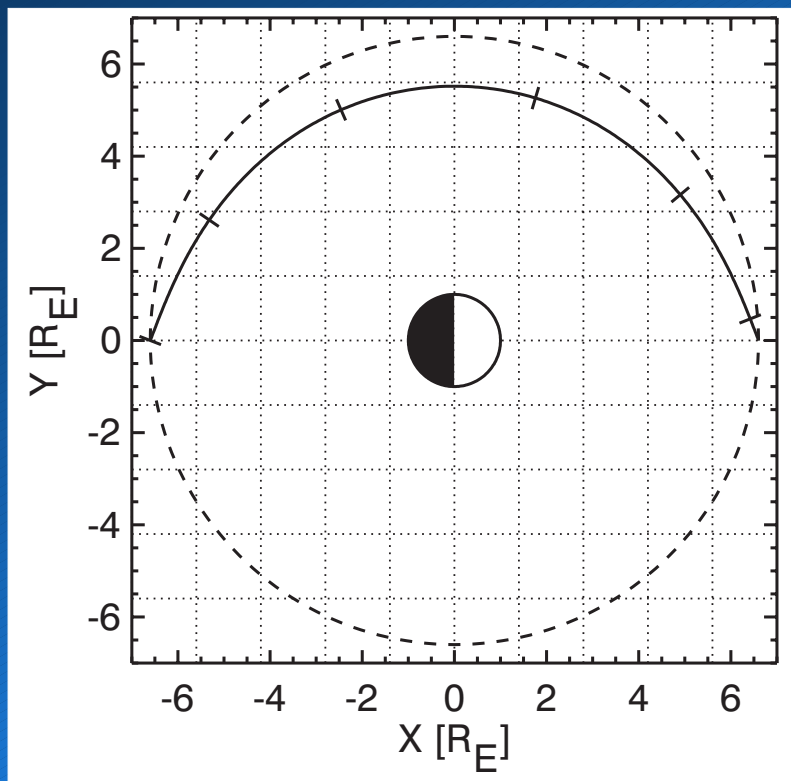


Weimer 96



# Geosynchronous Trajectories

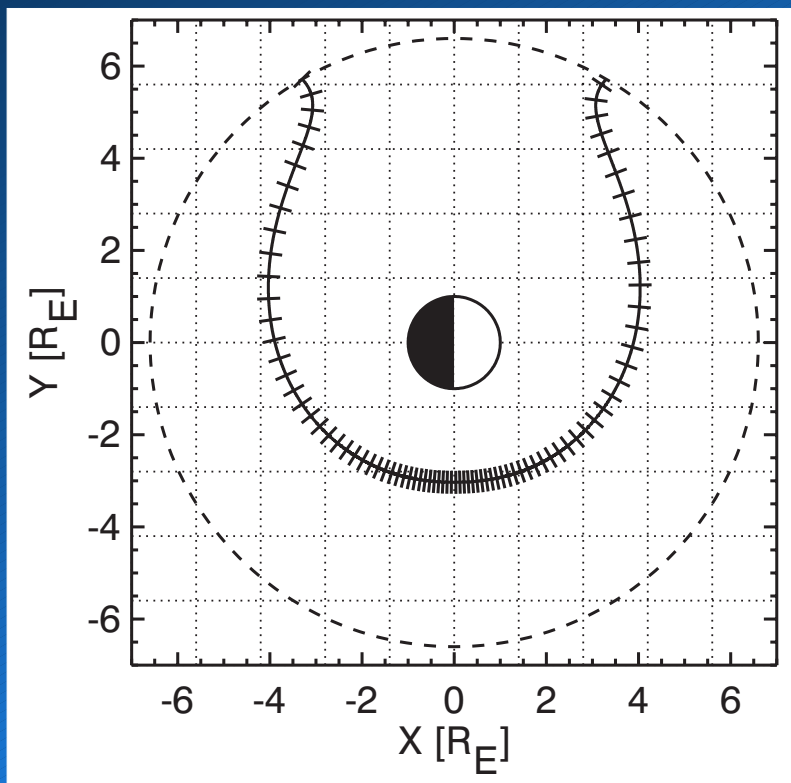
- Higher energies
- Example: 10 keV @  $6.6 R_E$ , 0 LT,  $K_p=3$ .



- Drift time:  $\sim 5$  hours.
- Simulated and observed **losses are comparable.**

# Near-Earth Trajectories

- Lower energies
- Example: 1 keV @  $6.6 R_E$ , 20 LT,  $K_p=3$ .



- Drift time:  $\sim 80$  hours.
- **Observed losses are much smaller** than simulations show.



## Summary

- Inversion algorithm was successfully tested on a testbed database obtained by forward-modeling drifts through a Chamberlain exosphere.
- MPA-data inversion shows large differences compared to the Chamberlain model in the near-Earth region.
- Inversions using other convection models produce similar results.
- These differences are due to lower-than-expected losses of lower-energy particles that nominally drift through the inner region.
- Possible implications:
  1. Actual hydrogen density may be lower than the Chamberlain model in the inner region predicts.
  2. There may be sources within the inner region.
  3. Drift paths don't actually penetrate that deeply. (More sophisticated convection models are needed, perhaps including temporal variations.)

